



RTM Amsterdam  
October 10th -11th, 2017



# 3D imaging of heterogeneous surfaces on laterite drill core materials

Henry Pilliere<sup>1</sup>, Thomas Lefevre<sup>1</sup>, Dominique Harang<sup>1</sup>, Beate Orberger<sup>2\*</sup>,  
Thanh Bui<sup>2</sup>, Anne Saloun<sup>2</sup>, Celine Rodriguez<sup>2</sup>, Cédric Duée<sup>3</sup>, Nicolas  
Maubec<sup>3</sup>, Xavier Bourrat<sup>3</sup>, Ali Mohammad Djafari<sup>6</sup>, Daniel Chateigner<sup>4</sup>,  
Saulius Grazulis<sup>5</sup>, Monique Le Guen<sup>2</sup>

- (1) Thermo Fisher Scientific, Artenay, France
- (2) Eramet, Trappes, France
- \* University of Paris-Sud, Orsay, France
- (3) BRGM, Orléans, France
- (4) University of Caen Normandie, Caen, France
- (5) Vilnius University, Lithuania
- (6) Centrale Supélec, Gif-sur-Yvette, France



# Contents

- Introduction
- Laser triangulation profilometer
- Preliminary results
- Conclusions and perspectives

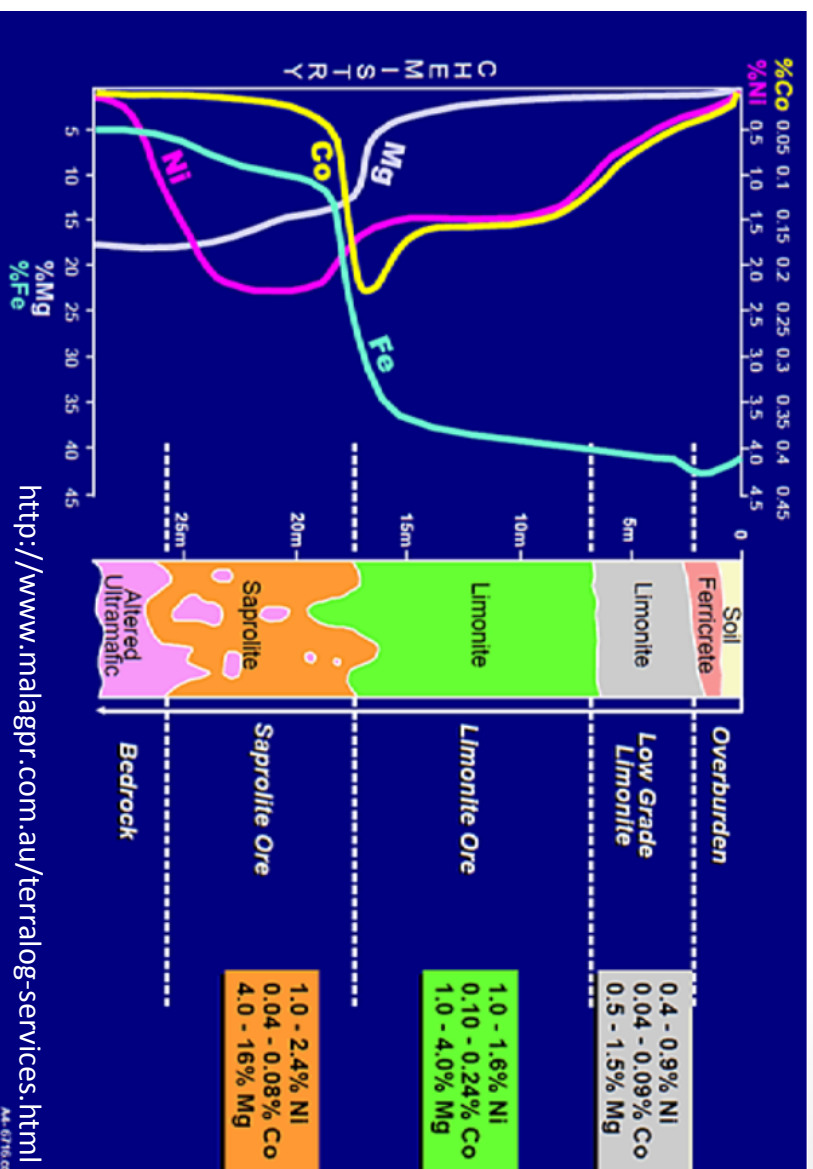


# Nickel laterites

Average chemical variations on the laterite profile:

- Ni resources:
  - Sulfide ores
  - Ni laterites
- Ni laterites
  - Constitute 60 – 70% of the world's Ni resources
  - Reach 60% of total Ni production in 2014
  - Contribute 20 – 30% of the total Co supply.

Butt *et al.*, 2013



- Three nickel laterite ore types, based on the dominant minerals hosting Ni:

Ores	Mean grades of Ni	Principle ore minerals	% of total Ni laterite resources	Position in lateritic profiles
Oxide	1.0 – 1.6 wt%	Goethite, absolane, lithiophorite	60%	Mid to upper saprolite and upwards to the plasmic zone
Hydrous Mg silicate	1.44 wt%	Serpentine, talc, chlorite, sepiolite	32%	Mid to lower saprolite
Clay silicate	1.0 – 1.5 wt%	Smectite, saponite	8%	Mid to upper saprolite

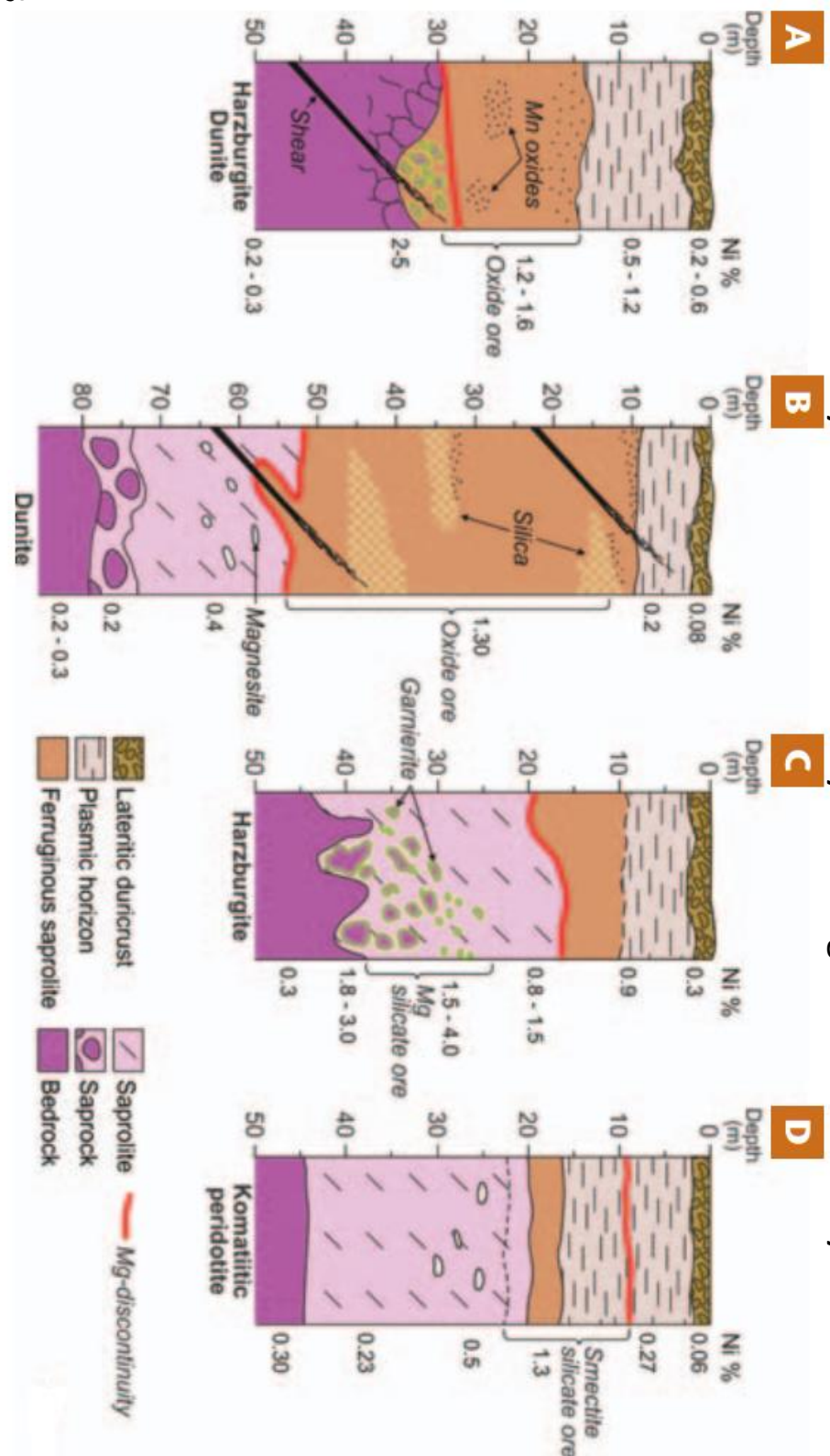
# Lateritic profiles

Oxide

Partly silicified oxide

Hydrrous Mg silicate

Clay silicate



Butt *et al.*, 2013

## OXIDE ORE

Goethite	Oxide	$\alpha\text{-(Fe}^{3+}\text{)O(OH)}$	2% Ni, 0.2% Co
Asbolane	Oxide	$(\text{Ni}^{2+}, \text{Co}^{3+})_x \text{Mn}^{4+}(\text{O, OH})_4 \cdot n\text{H}_2\text{O}$	16% Ni, >4% Co
Lithiophorite	Oxide	$(\text{Al, Li})\text{Mn}^{4+}\text{O}_2(\text{OH})_2$	1% Ni, ~7% Co

## CLAY SILICATE ORE

Nontronite	Smectite	$\text{Na}_{0.3}\text{Fe}_2^{3+}(\text{Si, Al})_4\text{O}_{10}(\text{OH})_2 \cdot n\text{H}_2\text{O}$	~4% Ni
Saponite	Smectite	$(\text{Ca}/2, \text{Na})_{0.3}(\text{Mg, Fe}^{2+})_3(\text{Si, Al})_4\text{O}_{10}(\text{OH})_2 \cdot 4\text{H}_2\text{O}$	~3% Ni

## HYDROUS MG SILICATE ORE

Ni lizardite - népouite	Serpentine	$(\text{Mg, Ni})_3\text{Si}_2\text{O}_5(\text{OH})_4$	6-33% Ni
7Å garnierite	Serpentine	Variable, poorly defined	15% Ni
Nimite	Chlorite	$(\text{Ni}_5\text{Al})(\text{Si}_3\text{Al})\text{O}_{10}(\text{OH})_8$	17% Ni
14Å garnierite	Chlorite	Variable, poorly defined	3% Ni
Falcondoite	Sepiolite	$(\text{Ni, Mg})_4\text{Si}_6\text{O}_{15}(\text{OH})_2 \cdot 6\text{H}_2\text{O}$	24% Ni
Kerolite-willemsseite	Talc	$(\text{Ni, Mg})_3\text{Si}_4\text{O}_{10}(\text{OH})_2$	16-27% Ni
10Å garnierite	Talc	Variable, poorly defined	20% Ni

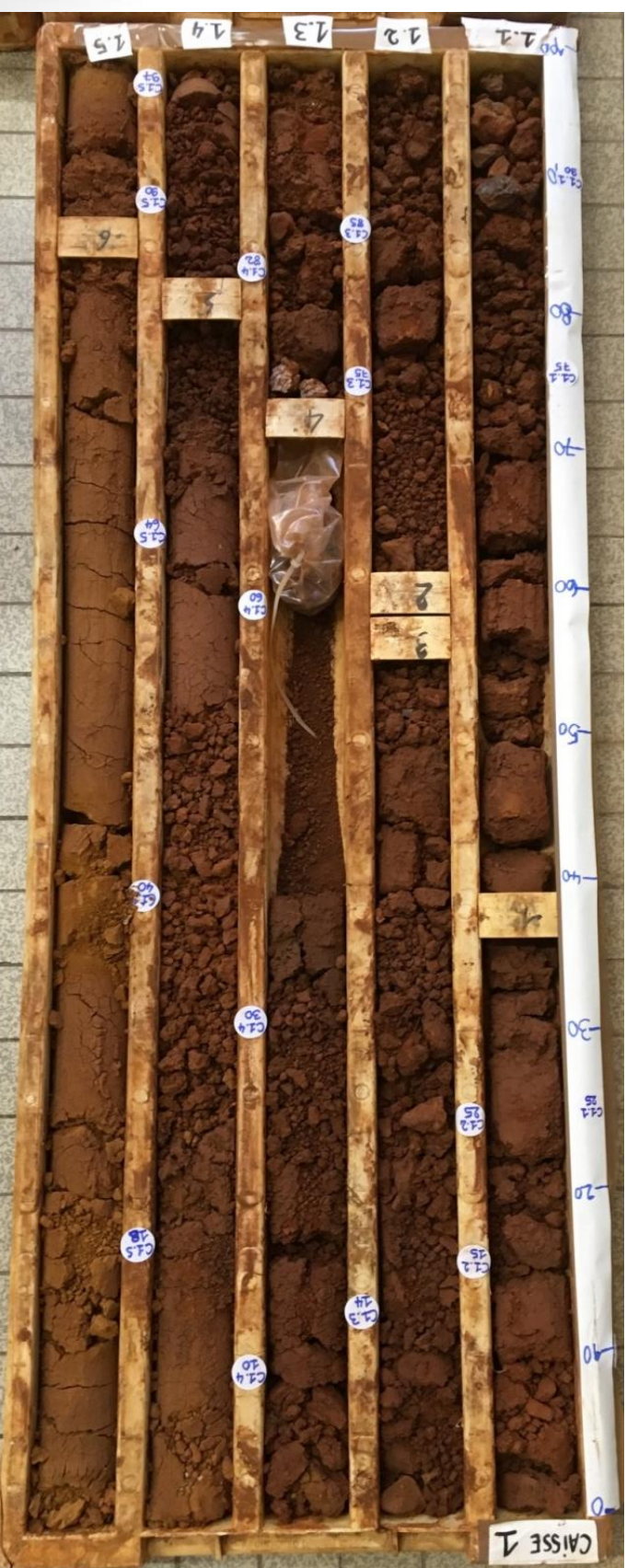


# Observations on drill cores





# Observations on drill cores





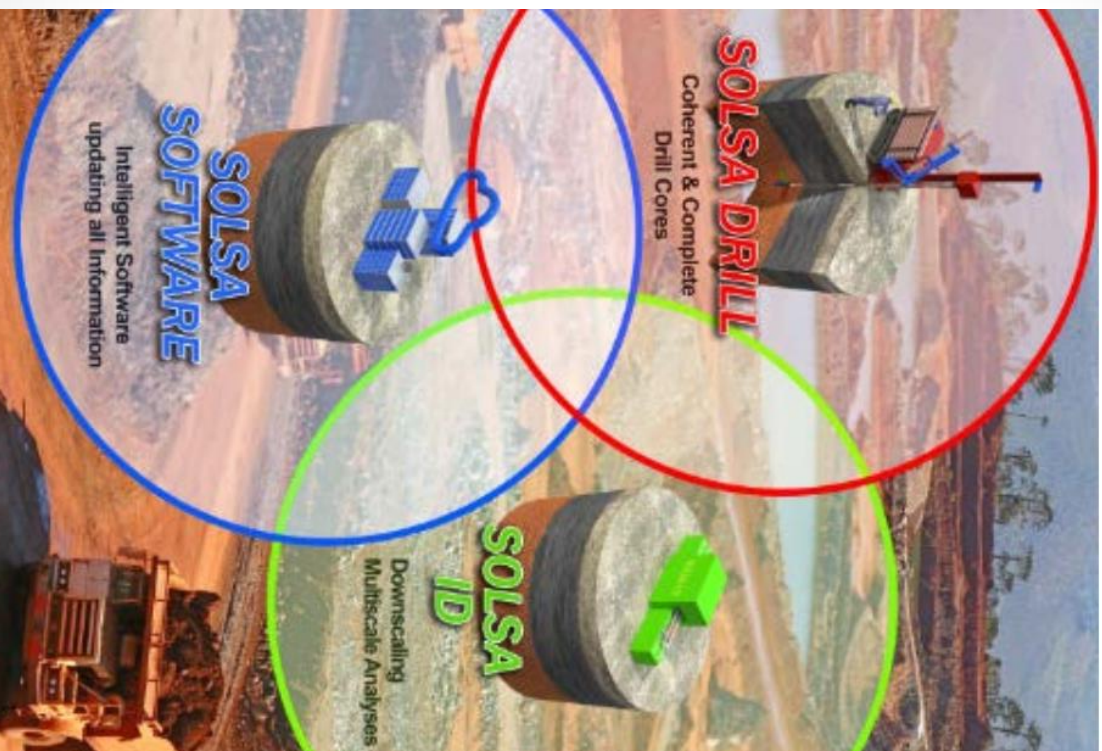
## To develop an imaging system of drill cores

- Need to take into account the following features/information:
  - Depth, drilling speed
  - Textures:
    - RGB camera, profilometer
    - Roughness
    - Profilometer
  - Hardness, porosity:
    - Drilling system, hyperspectral cameras, RGB camera(?)
  - Principal ore minerals:
    - Hyperspectral imaging: diagnostic absorption features,
  - Ni content:
    - Portable XRF





# SOLSA



SOLSA ID 1  
Analyse & Identification in **laboratory conditions**  
-> **Test configurations to be used for ID 2**

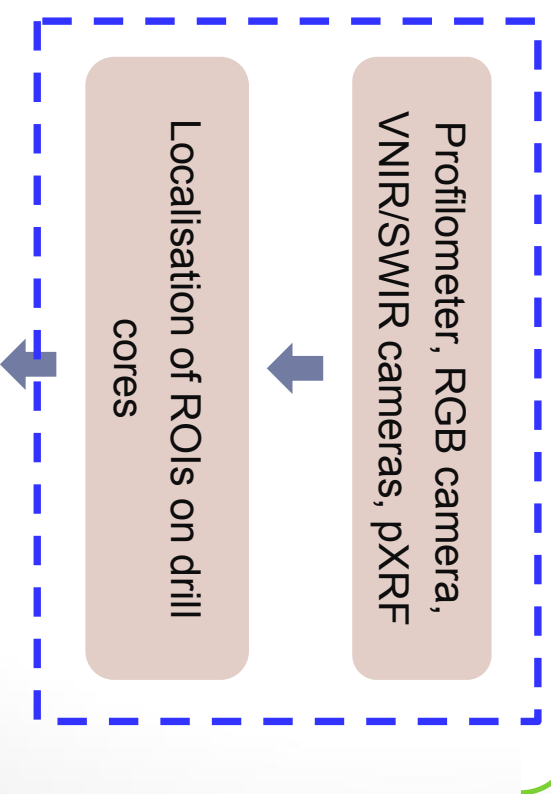
SOLSA ID 2  
Analyse & Identification in  
**field and industrial applications**

SOLSA ID 2A,  
measurement

SOLSA ID 2A,  
processing

SOLSA ID 2B,  
measurement

SOLSA ID 2B,  
processing

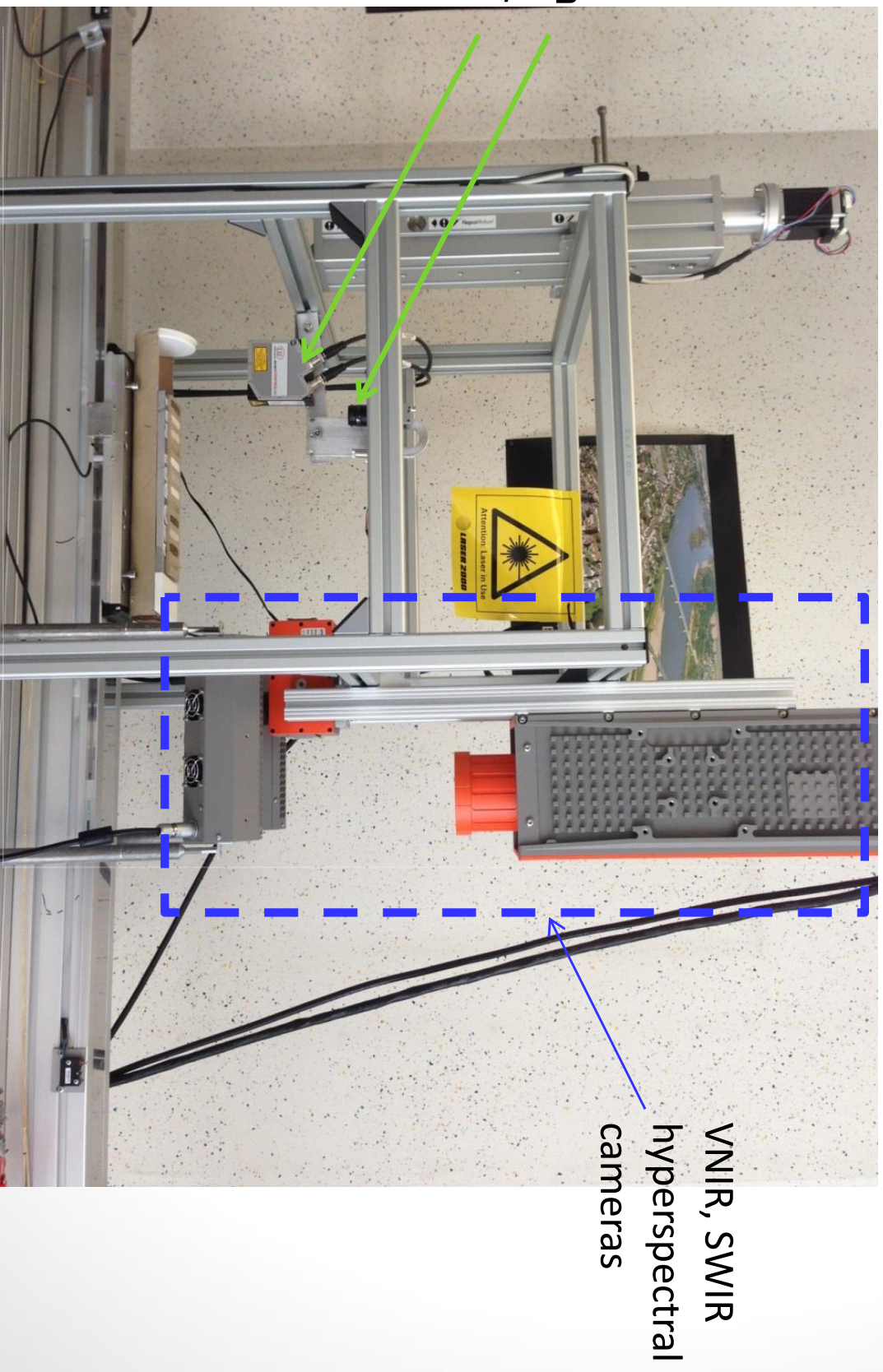




# ID2A scanning prototype

**Goal:** to built a system for scanning drill cores by imaging. Two results are expected:

- to know the outer shape of the core, in order to help for automatic positioning of the analytical system.
- to identify regions of interest on the surface of the core





# Work in progress

- Hyperspectral imaging: to identify the principal ore minerals, (crystallinity)
  - Building spectral library: collection of spectra of pure minerals (endmembers)
  - Spectral classification: to classify different minerals using their spectra
    - A classification method based on Support Vector Machines has been developed.
  - Spectral unmixing: to infer pure spectral signatures (endmembers) and their corresponding proportions (abundances)
    - A method of sparse unmixing based on a spectral library has been developed.
- Profile data (profilometer) and RGB images:
  - To quantify the roughness of the surface
  - To obtain the structure of grains and texture information of the drill cores
- To support hyperspectral interpretation and pXRF analysis



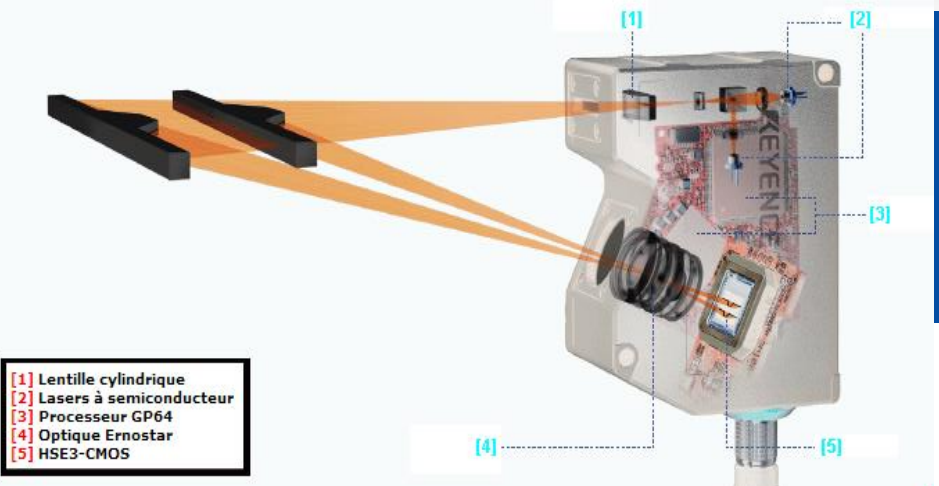




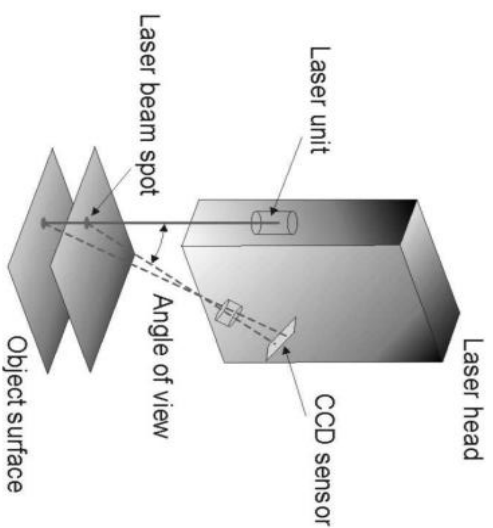
# Contents

- Introduction
- **Laser triangulation profilometer**
- Preliminary results
- Conclusions and perspectives

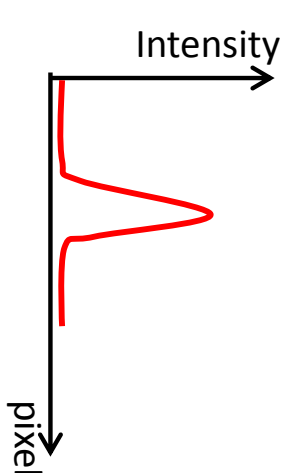
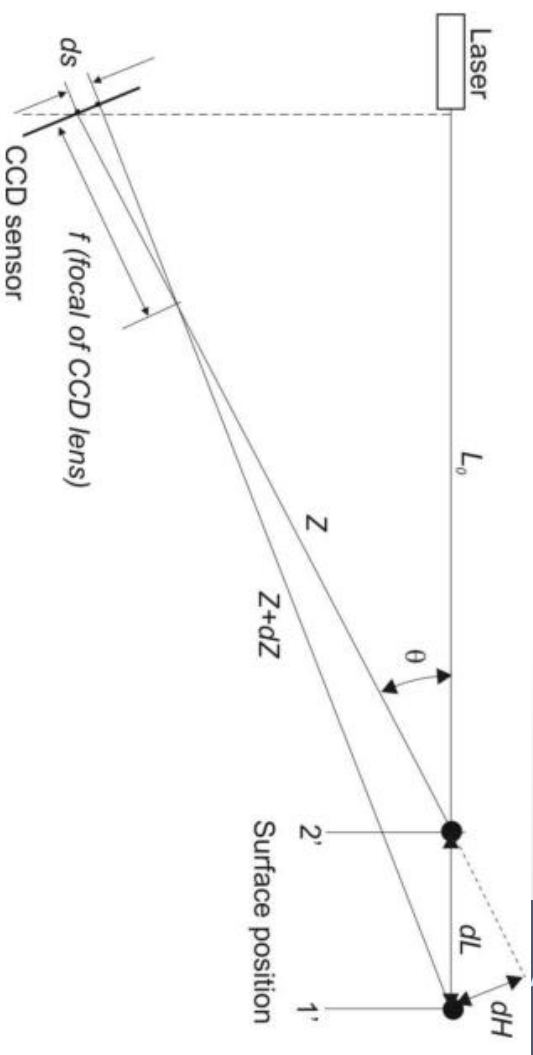
# Triangulation profilometer principle



- [1] Lentille cylindrique
- [2] Lasers à semiconducteur
- [3] Processeur GP64
- [4] Optique Ernstar
- [5] HSE3-CMOS



When the laser beam illuminates the surface of an object, the illuminated point is projected, towards the focal depth of the camera, onto the image CCD sensor.



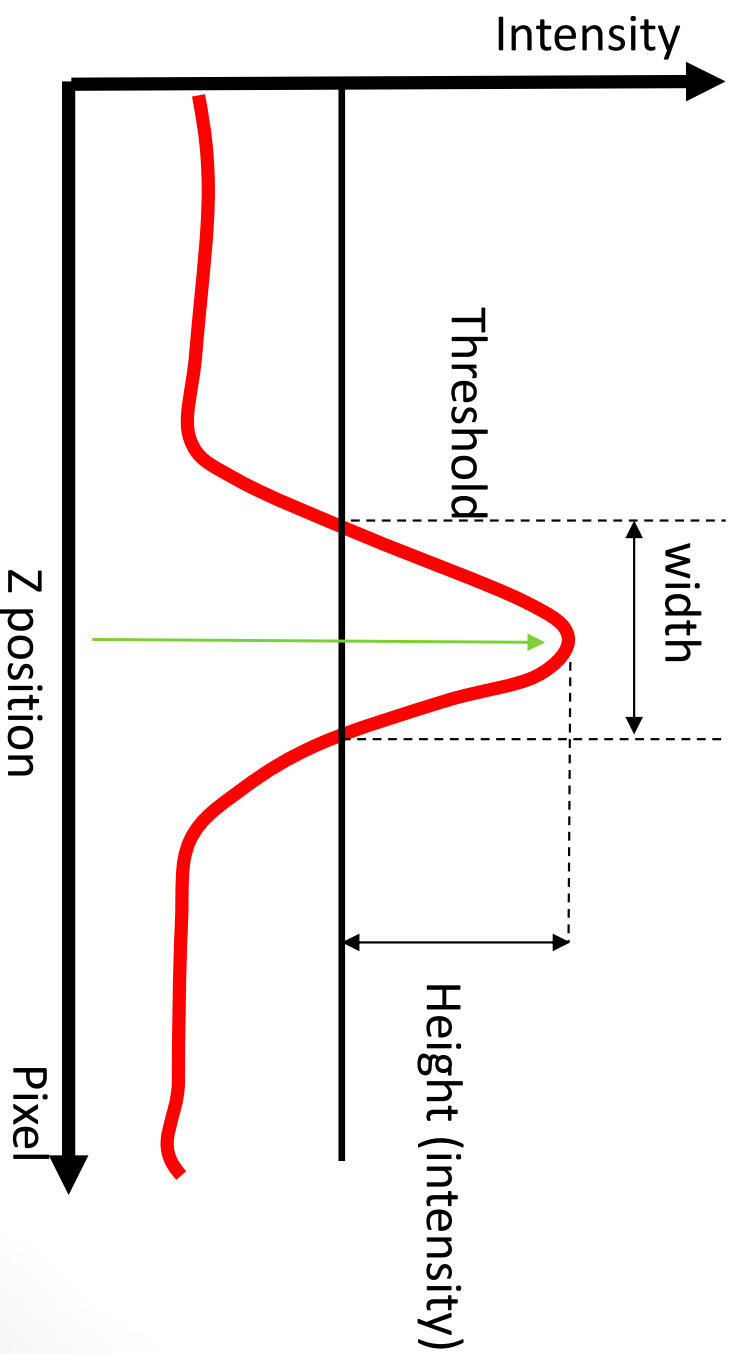
## Non-contact laser triangulation

The position of the laser spot on the CCD sensor is related to the position of the laser spot on the object surface. The measurement sensitivity:

$$\frac{ds}{dZ} = \frac{f}{Z} \sin \theta$$

# Description of the reflected signal

- **Threshold:** Actual threshold
- **Height (intensity):** Maximum intensity of the reflection above the threshold
- **Position (in pixel)** corresponds to the pixel row on the CMOS sensor with maximum intensity. This is indicative of the surface profile.
- **Width:** The width of reflection in pixel. This value is indicative of the signal diffusion.







# Conveyor and imaging

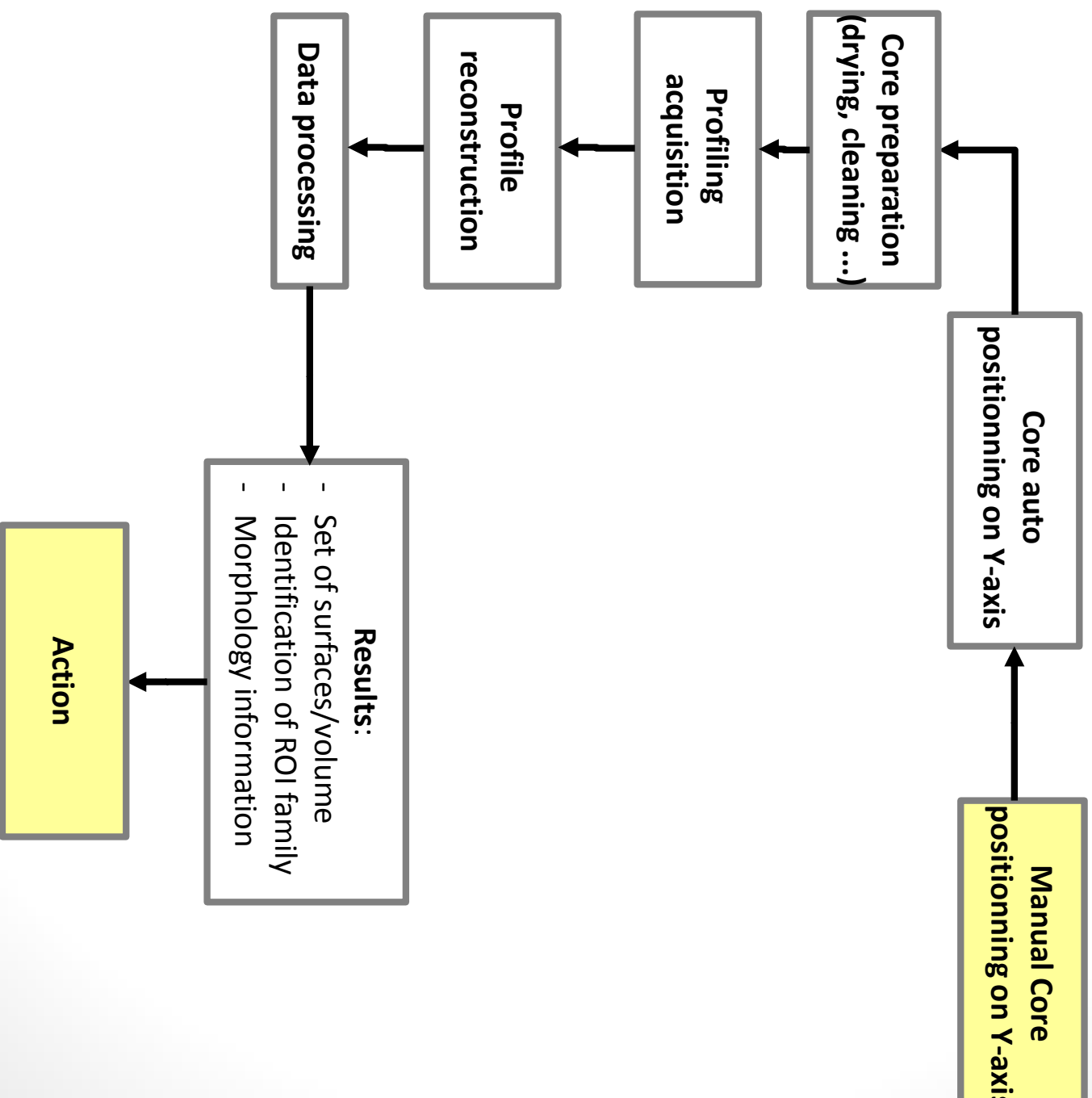
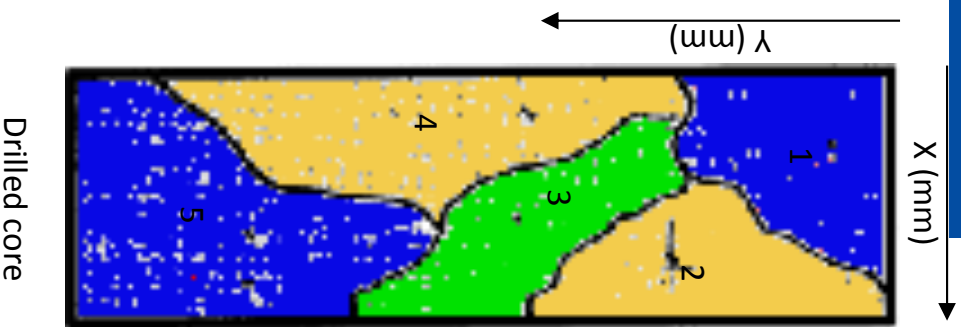
Imaging part is composed of:

- Conveyor (along Y-axis)
- Profilometer (x, y, z, Intensity, width)
  - Need to movement of conveyor to reconstruct the surface profile
- RGB camera: (x, y, RGB)
  - No z information





# Scheme of profiling processing





# Contents

- Introduction
- Laser profilometers
- Preliminary results
- Conclusions and perspectives

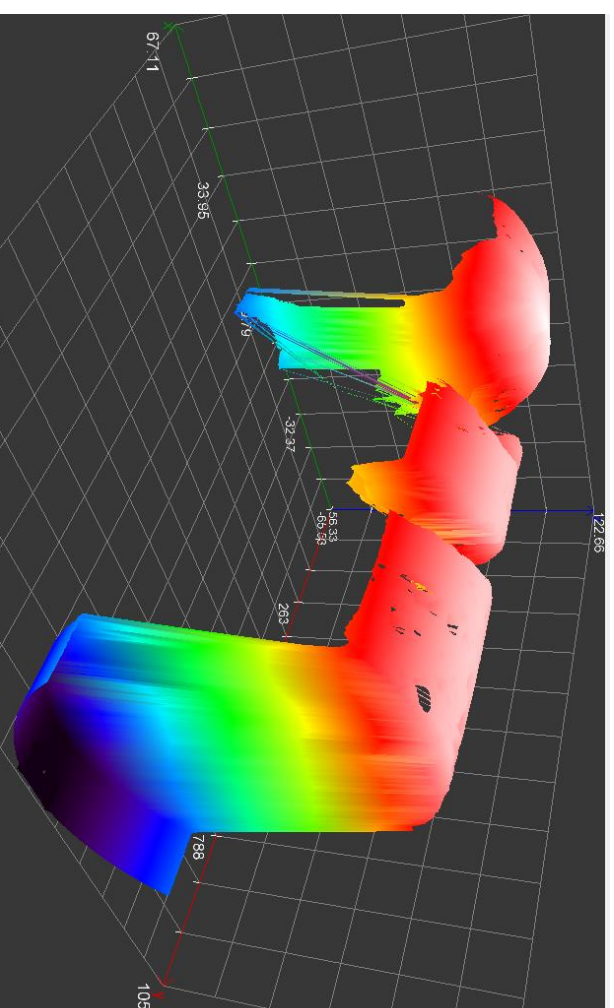


# Example: cylindrical surface of breccia



Sample « breccia » series 2

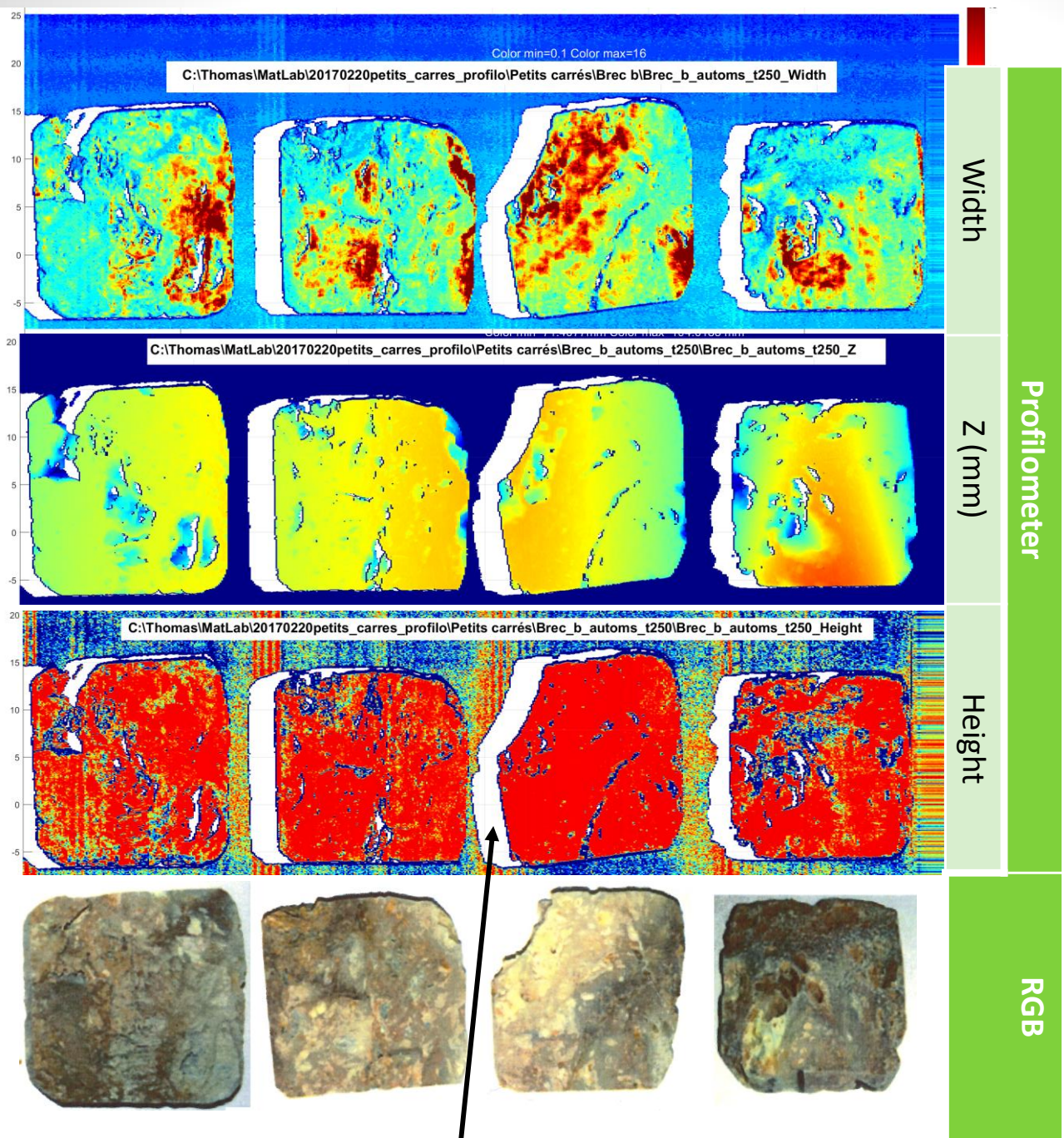
- Performing:
- Real surface reconstruction
  - Analysis of defects (cracks and porosity)



Sample « breccia » XYZ profile



# Example: surfaces effect on breccia



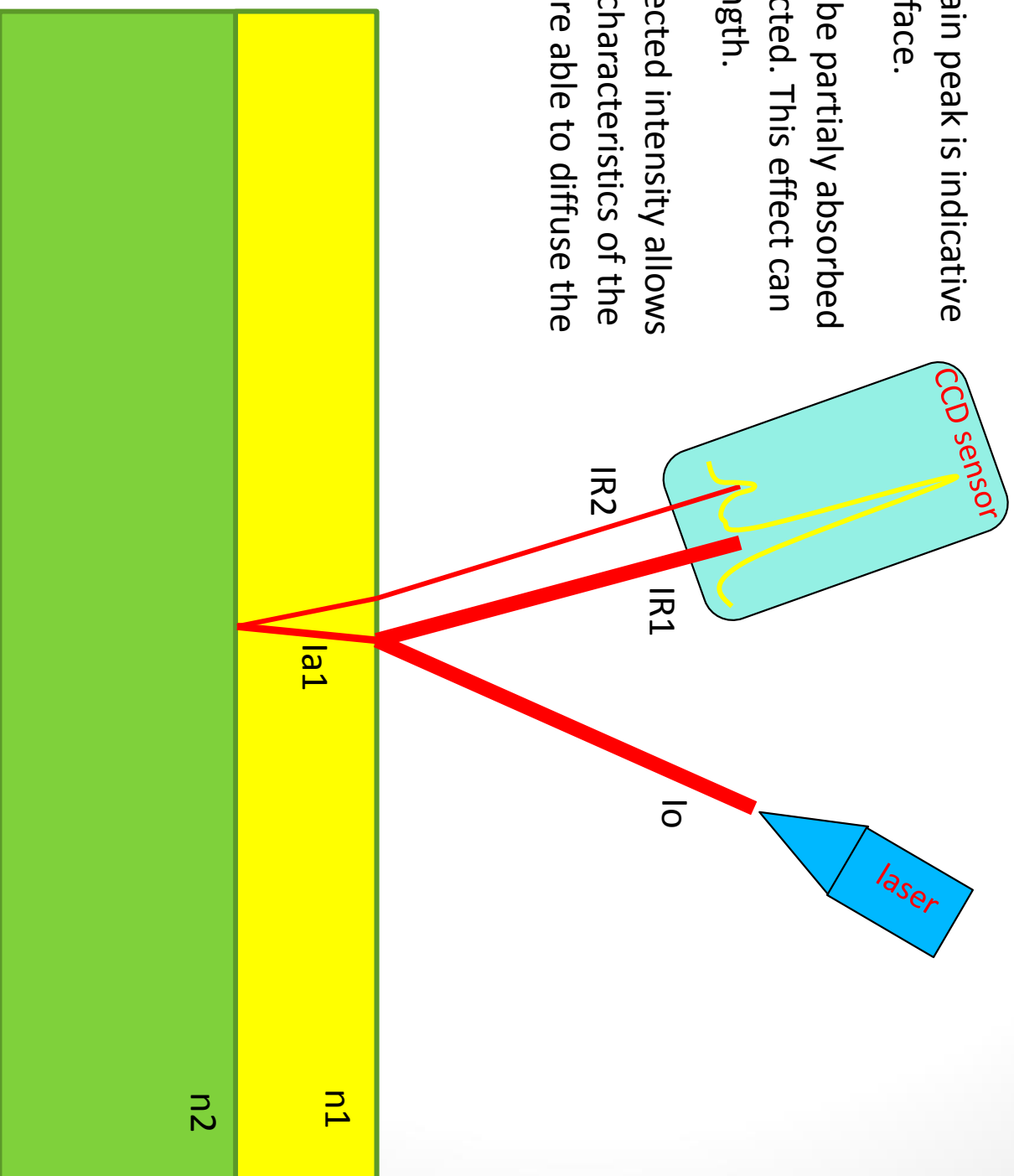
- Z and Height: no effect on mineralogy
- Width: effect on mineralogy

shading



# Profiling principle: interaction light/matter

- The deviation of the main peak is indicative of the height of the surface.
- The incident beam can be partially absorbed by the surface, or refracted. This effect can depend on the wavelength.
- The analysis of the reflected intensity allows to quantify the optical characteristics of the surface. All interfaces are able to diffuse the incoming light.



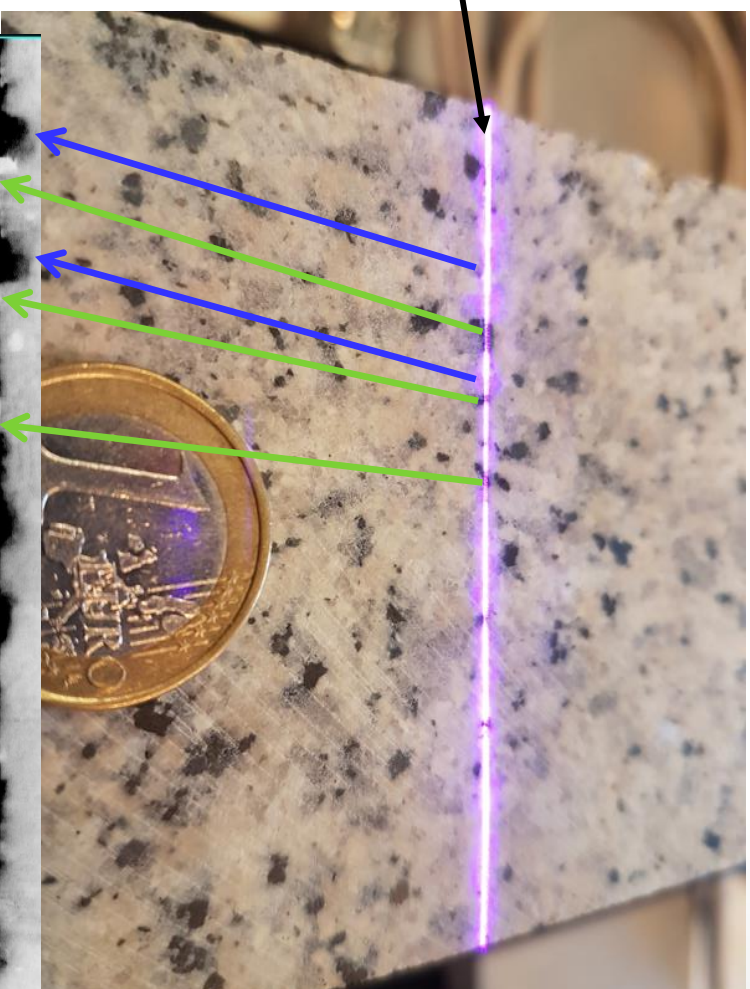


# Example: flat surface of granite

Laser line (405nm) on a flat surface of a granite rock.

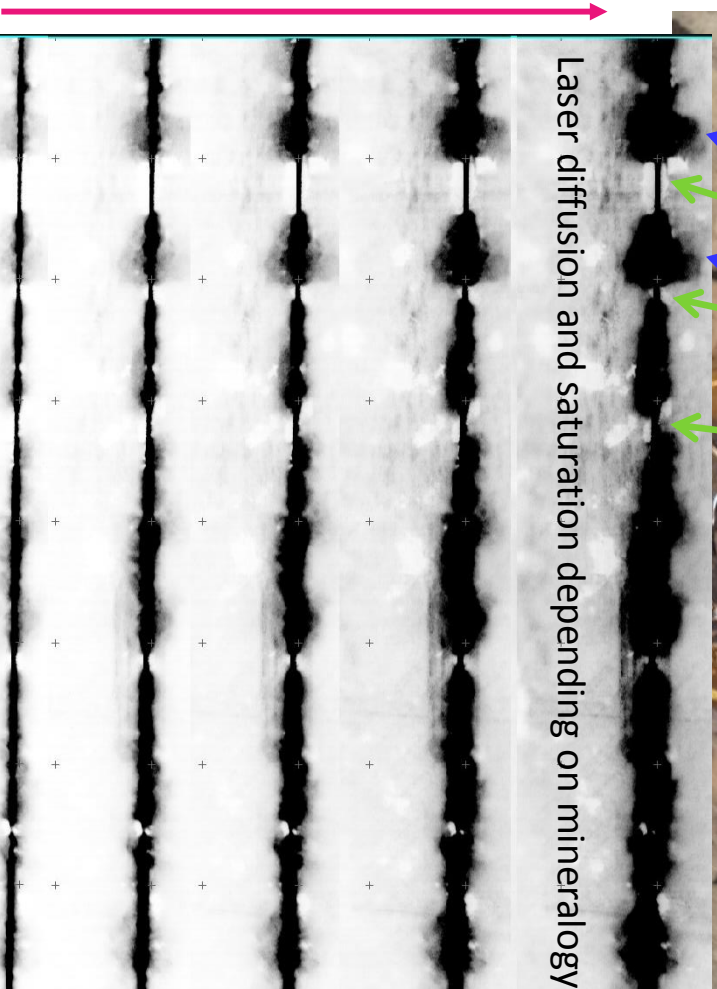
Granit is mainly composed by 2 transparent minerals (quartz and felspar) and highly reflected mineral (biotite, in black)

Compared to a simple lightening, the laser allows to enhance the optical properties of the mineral, and intensity quantification can be done.



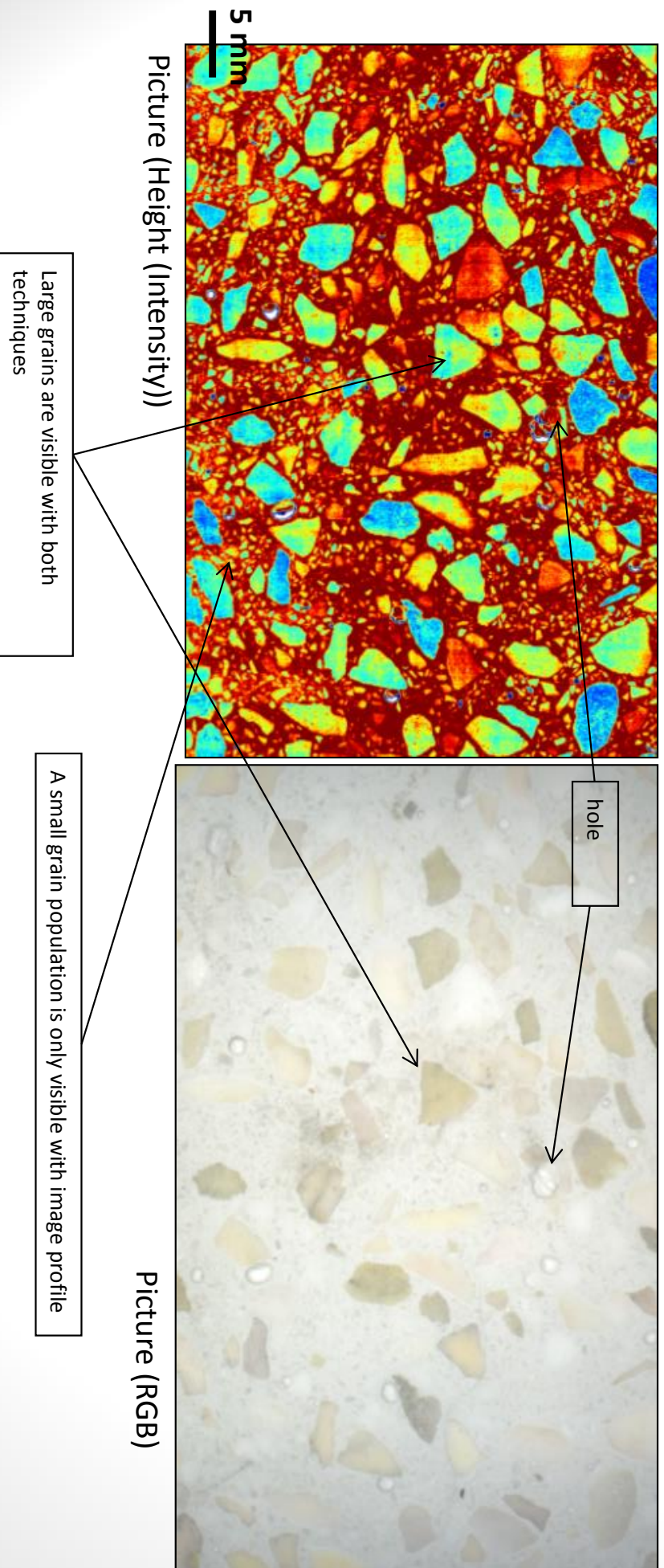
Laser diffusion and saturation depending on mineralogy

Threshold decreasing



# Mapping grains

- Comparison between profilometry and RGB images on an heterogeneous sample.
- There are more informations in the image profile intensity than in RGB image
  - 3 surface families:
    - Large grain
    - Small grain



# Mapping grains

Observation : Picture (z) allows to identify clearly porosity and cracks



Image analysis of picture (z) will allow to measure roughness.

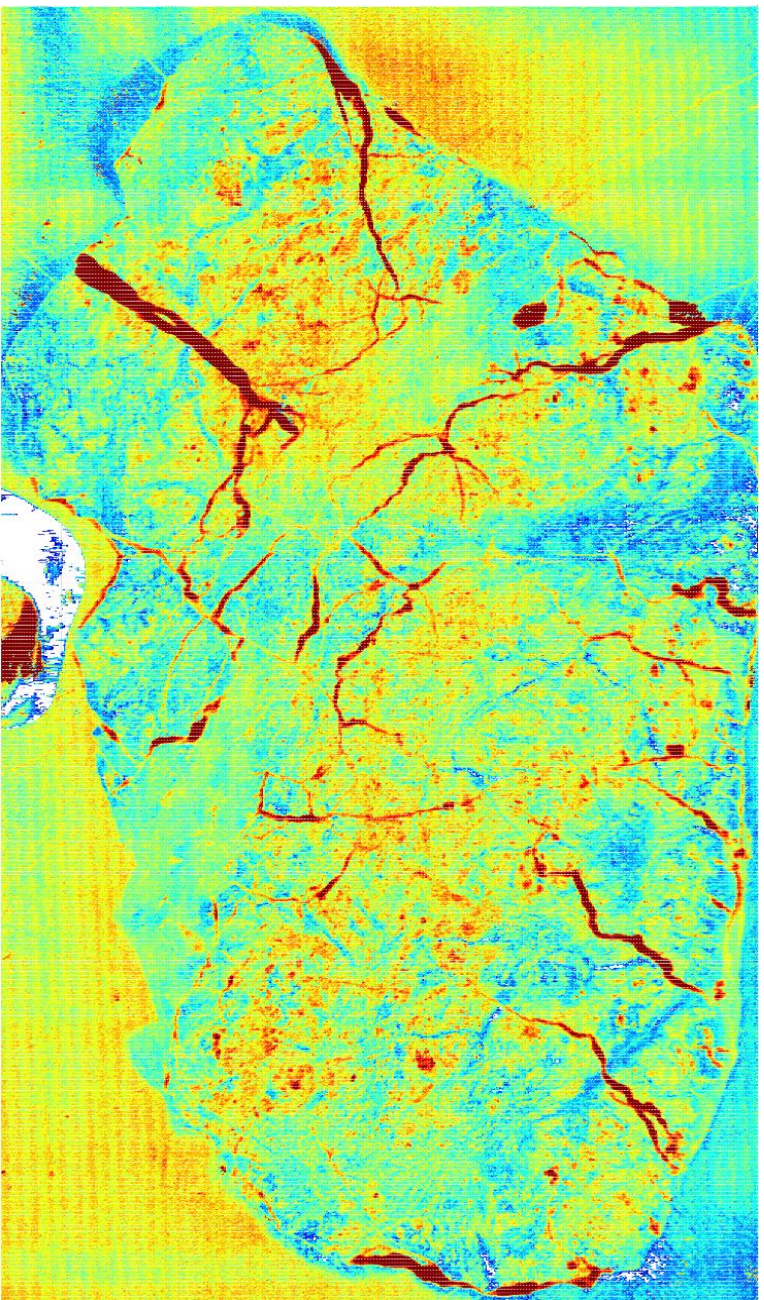




Serpentined sample  
(saprolite level on  
peridotite bed rock):



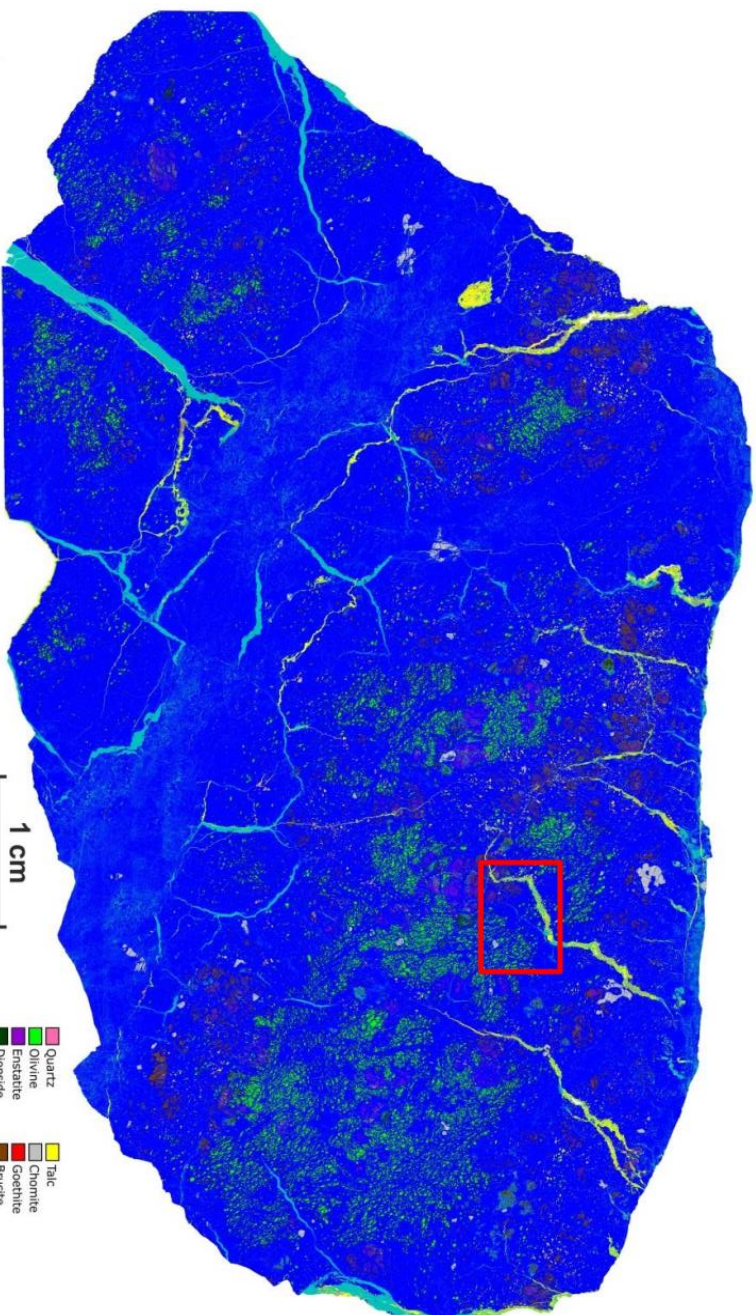
Width







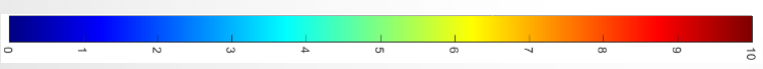
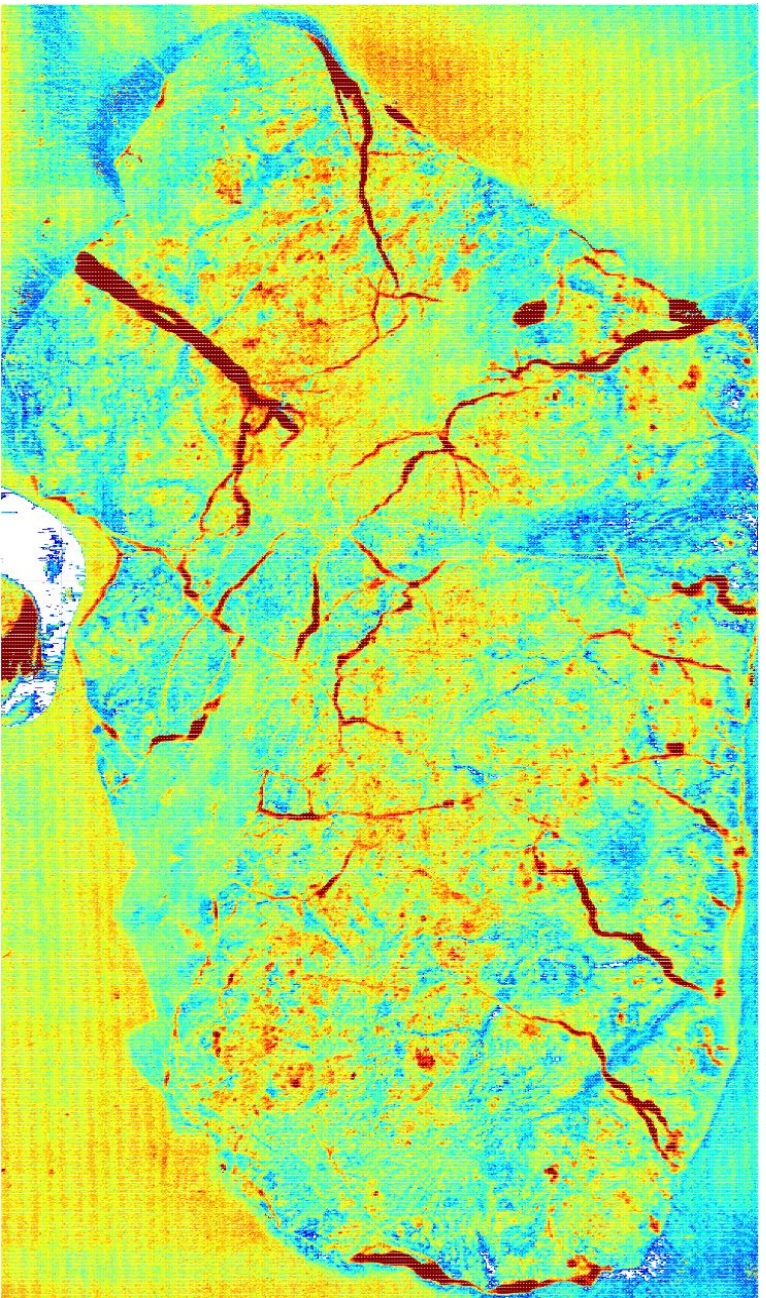
Serpentined sample  
(saproelite level on  
peridotite bed rock):



Gemscan mineralogical mapping

- Quartz
- Olivine
- Enstatite
- Dioopside
- Amphibole
- Serpentine Mg
- Serpentine Fe
- Talc
- Chromite
- Goethite
- Brucite
- Dolomite
- Other minerals

Width





# Contents

- Introduction
- Laser triangulation profilometer
- Preliminary results
- Conclusions and perspectives



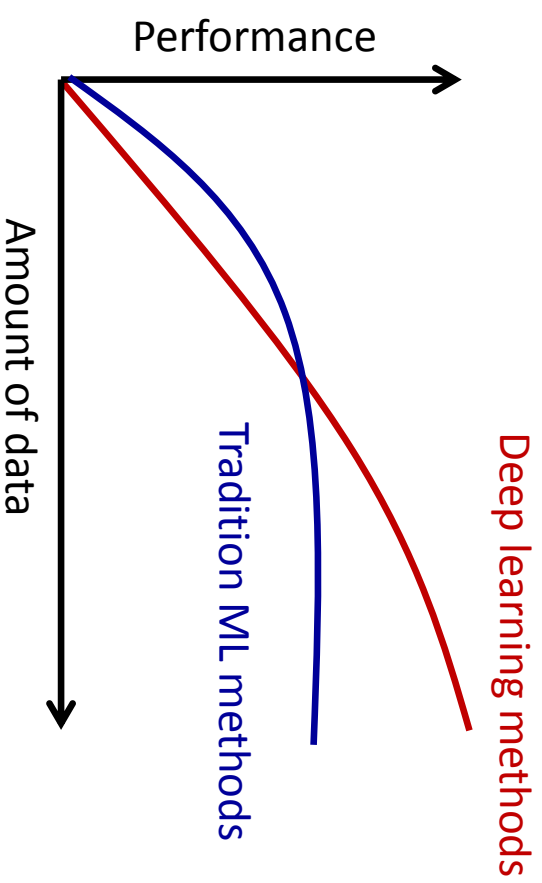
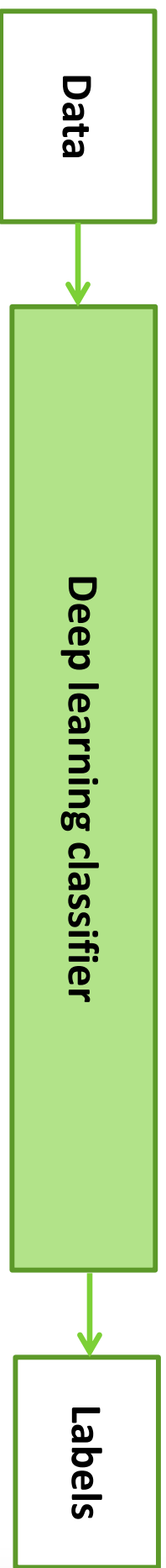


# Conclusions and perspectives

- Profilometry imaging brings a volumetric dimension that cannot be done with classical RGB.
- Morphologic parameters can be quantified better than classical RGB.
- Mineralogical contour is improved.
- Data processing routines are under construction.
- Texture analysis will be done using RGB images
- Hyperspectral imaging (in progress):
  - Collecting endmembers (building hyperspectral library)
  - Evaluating hyperspectral classification and unmixing techniques on data acquired from harzburgite, dunite and bauxite samples



# Conclusions and perspectives





Thank you for your attention!



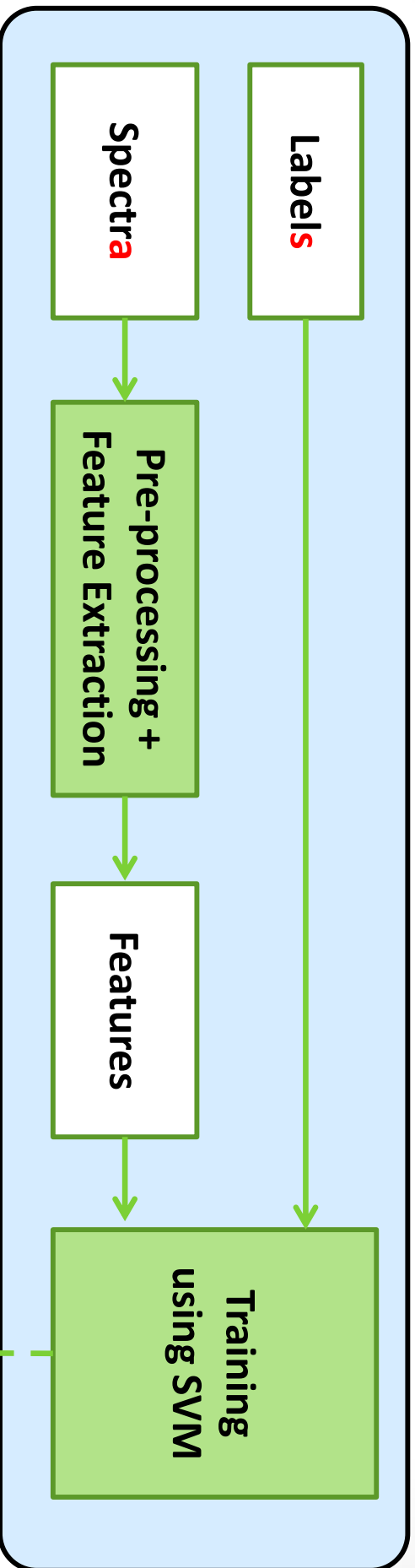


# VNIR/SWIR camera parameters

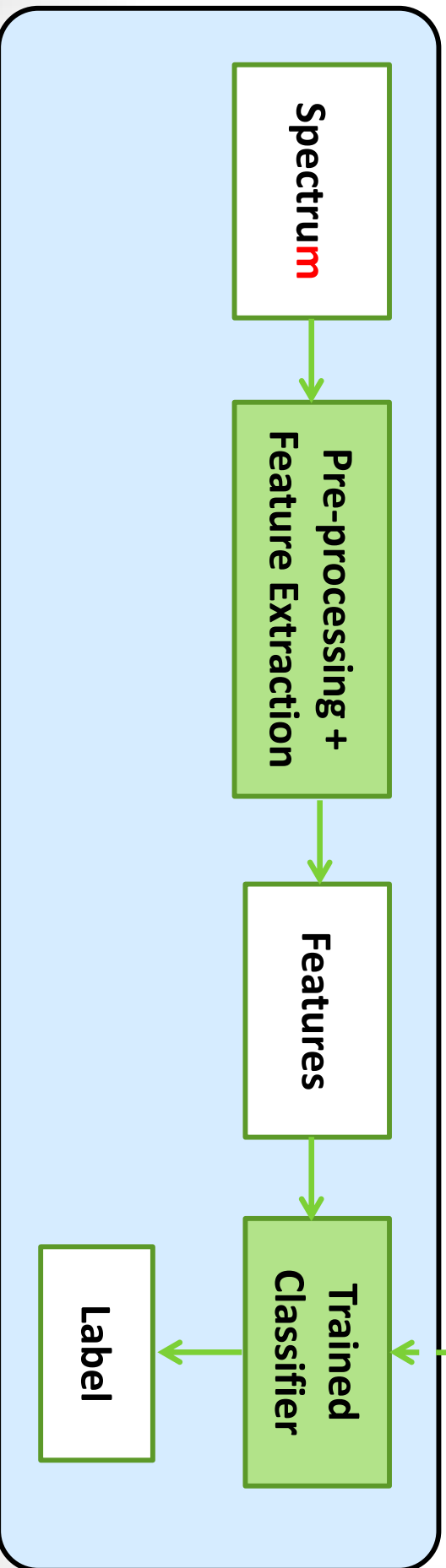
Parameters	FX10 VNIR	SWIR OLESS30
Spectral range (nm)	400 - 1000	1000 - 2500
Spectral bands	224	288
Spectral FWHM (nm)	5.5	12
Spatial sampling	1024	384
Field of View (degree)	38	17
Maximum frame rate (fps)	330	450
Exposure time range (ms)	0.1 – 20	0.1 – 20
Aperture	1.7	2
Focal length (mm)	15	30
Measurement distance (m)	0.118	0.316
Field of View (mm)	81.26	94.45
Spatial resolution (um)	79.36	245.97
Depth of Field (mm)	1.91	9.64

# Spectral classification

## Training phase



## Prediction phase



# Sparse unmixing methods

$$Y = AX$$

OBSERVED IMAGE

$y_1$	$y_2$	$y_3$	...	...	...	...	...	$y_n$
-------	-------	-------	-----	-----	-----	-----	-----	-------

SPECTRAL LIBRARY

$a_1$	$a_2$	$a_3$	...	...	...	...	...	$a_m$
-------	-------	-------	-----	-----	-----	-----	-----	-------

$\times$

MATRIX OF FRACTIONAL ABUNDANCES

	$x_1$	...	
$x_1$	$x_2$	...	
$x_2$			
$\vdots$	$\vdots$	$\vdots$	$\vdots$
$x_j$			
$\vdots$			
$x_m$			

$Y$   
 $L \times n$

$A$   
 $L \times m$

$X$   
 $m \times n$

$$\min_X \|AX - Y\|_F^2 + \lambda \|X\|_{2,1}$$

subject to:  $X \geq 0, \mathbf{1}X = 1$





$\mathbf{X}(m \times n)$

# Unmixing methods

CLSUnSAL

(Collaborative sparse unmixing by variable splitting and augmented Lagrangian):

$$\min_{\mathbf{X}} \|\mathbf{A}\mathbf{X} - \mathbf{Y}\|_F^2 + \lambda \|\mathbf{X}\|_{2,1}$$

subject to:  $\mathbf{X} \geq 0, \mathbf{1}\mathbf{X} = 1$

SUnSAL

(Sparse unmixing by variable splitting and augmented Lagrangian):

$$\min_{\mathbf{X}} \|\mathbf{A}\mathbf{X} - \mathbf{Y}\|_F^2 + \lambda \|\mathbf{X}\|_{1,1}$$

subject to:  $\mathbf{X} \geq 0, \mathbf{1}\mathbf{X} = 1$

FCLS

(Fully constrained least squares):

$$\min_{\mathbf{X}} \|\mathbf{A}\mathbf{X} - \mathbf{Y}\|_F^2$$

subject to:  $\mathbf{X} \geq 0, \mathbf{1}\mathbf{X} = 1$

The optimization is based on the alternating direction method of multipliers (ADMM).

Bioucas-Dias *et al.*, 2010

lordache *et al.*, IEEE Trans, 2014

Afonso *et al.*, IEEE Trans, 2011